Comparison of a Persistent Random Walk to 3D Chemo taxis in MDA-MB-231 Cancer Cells

Cameron Thayer-Freeman

Advisor: Dr. Bo Sun

2015

Abstract

This research specifically examines the collective motion of populations of MDA-MB-231 breast cancer cells under the influence of a chemo-attractant gradient. Their motion is compared to the mathematical model of a persistent random walk, measuring the persistence bias of the cells from their autocorrelation function and applying to the mean squared distribution function predicted by the persistent random walk model. The motion of cells within the population is also analyzed; comparing free and caged cancer cell motion to the model of a persistent random walk. The results show strong evidence towards the conclusion that the collective motion of breast cancer cells does not fit into the model of a persistent random walk.

Table of Contents

List of Figures and Equations

Chapter 1

Chapter 2

Chapter 3

Chapter 1 – Introduction

1.1 – Motivation and Objective

Being able to accurately model and predict the behavioral motion of cancerous cells is key to further understanding cancer metastasis. Many current models for cellular motion, previously applied to other types of cells, don't work when modeling cancer cell motion.

The main focus of this research is to study the physics of the cell's migratory patterns as they move through tissue, between their point of origin and their final destination in the blood vessels. For about 30 years the primary physical model used to describe most active cell motion is that of a persistent random walk.[1] Recent research though, performed by Pei-Hsun Wu et al, shows evidence towards the conclusion that this model does not accurately fit the motion of endothelial cancer cells. Their research only examined individual cells and did not look into averaged motion over larger populations.[2] The model of a persistent random walk does not take into account the influence of a gradient, and as most cancerous cell metastasis is primarily influenced by the presence of a chemical bias, an updated model may be needed to describe their motion.[3]

This research studies the motion of populations of MDA-MB-231 breast cancer cells when directed by a chemical gradient, and analyzes individuals within the population. It analyzes the results the autocorrelation function mean squared displacement, and compares them to what the model of a persistent random walk would predict.

1.2 – Cancer Metastasis

Cancer occurs when healthy bodily cells suffer some damage to their genetic code which prevents external regulation of their motion and replication patterns.[4] Without any mechanisms of control the cells become an invasive parasite in the body. Most cancers though only become a serious concern when they metastasize, migrating away from their tumor of origin. Metastasis, by definition, is the spread and migration cancerous cells away from their tumor of origin.[5] The chance of metastasis occurring depends upon the type of cancer and where the cancer forms. In the case in which it occurs, cells actively spread away from their tumor, their overall direction of motion being highly influenced by the nutrient concentration in the surrounding tissue. Figure 1.1 present a theoretical model breast cancer cell metastasis. As the cells move through the surrounding tissue, often guided by a chemical attractant, they eventually end up in blood vessels where they are carried off by the body's circulatory system to other parts of the body to form more tumors.[6] This research specifically examines the earliest stage of cancer metastasis, after they move away from their tumor and before they reach any blood vessels.

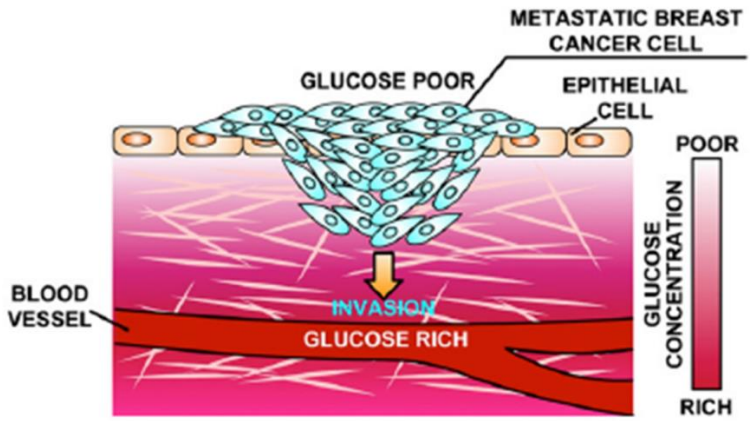

Figure 1.1 A theoretical model of metastatic breast cell migration through surrounding breast tissue.

1.3 – Modeling Cell Motion

1.3.1 – Persistent Random Walk

For over 30 years the collective and individual motion of most cells has been described by the application of a statistical random walk to their motion. A simple or isotropic random walk by definition is a succession of random steps, with no clear direction or bias. The model of a simple random walk has been used to model molecular motion in gases, foraging patterns of animals, and even fluctuations in the stock market.[1] Due to the statistical nature of random walks, the pattern does not become obvious until multiple walks are carried out. Each walk may take its own direction, but when averaged out the overall direction will always be approximately zero. Figure 1.2 demonstrates an example of multiple one-dimensional random walks generated by a computer simulation. Though the multiple walks take several different paths, the average centers around zero.

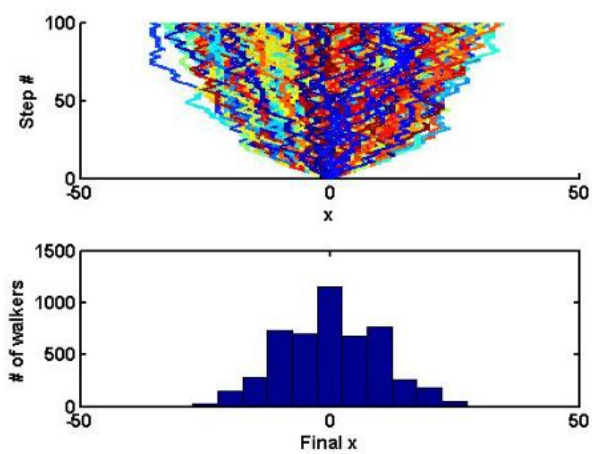

Figure 1.2 An example of a computer generated statistical random walk. The first plot represents a collection of 1D random walks, with the x-axis representing the generated value of the walk, and the y-axis representing the number of successive steps in the walk. The second plot is a histogram of the number of random walks carried out and what the final values of the walks were.

A persistent random walk (PWR), otherwise known as a biased random walk, is a succession of random steps in which the probability to move in one direction is greater than the others.[7] The PRW is often used to model active cell chemo taxis, as when the cells move, the directionally of their motion is being influenced by an external bias. The PWR model of cell motility is derived from a differential equation describing the motion of a self-propelled cell

$$\frac{dv}{dt} = -\frac{1}{P}v + \frac{S}{\sqrt{P}}\boldsymbol{w} \text{ (Eq. 1)}$$

where t is time, v is the cell velocity, P is the persistence time, S is the speed of the cell, and $\boldsymbol{w}$ is the random vector of a Wiener process.[8] When analyzing cell motility, a key characteristic of the PRW model is the mean squared displacement (MSD), which is essentially a measured of how much the system the cells explored as a function of time. According to the PRW model, the MSD is given by the function

$$MSD(\tau) = nS^2P^2\left(e^{-\frac{\tau}{P}} + \frac{\tau}{P} - 1\right) \text{ (Eq. 2)}$$

where n is the dimension of the extracellular space, and τ is the time lag between positions of the cell.[9] When taking into account observational error in measurements, according to previous research, Eq. 2 becomes

$$MSD(\tau) = nS^2P^2\left(e^{-\frac{\tau}{P}} + \frac{\tau}{P} - 1\right) + 4\sigma^2 \text{ (Eq. 3)}$$

where σ^2 is the variance of observation noise in cell position.[2] Another key characteristic of the PWR model is that the autocorrelation function of the velocity vector exhibits a single exponential decay

$$< v(\tau)v(0) >= \frac{nD}{P}e^{-\frac{\tau}{P}} \text{ (Eq. 4)}$$

where D is the diffusivity of the cell. The primary objective of this research will be to calculate the normalized autocorrelation of an MDA-MB-231 cancer cell population, fit Eq. 4 to experimental results, and use the fit to calculate what the persistence bias is. That value is then used to create a plot for Eq. 3 and compare it to experimental results. This will give insight in how accurately the PWR model describes endothelial cancer cell motion.

1.3.2 – Persistent Random Walk in Individual vs. Collective Cell Motion

Recent research suggests that cancer metastasis may be a collective effort carried out by multiple cells moving as groups. Cancer research by Bo Sun *et al.* showed that breast cancer cells during metastasis will often follow a small number of “leader” cells that pave a way through the extracellular matrix.[10] Research such as this suggests a level of complexity in collective cancer

cell motion that the theory of a PRW cannot model. It also suggests a change in cell behavior when they are closer to each other. This research will also examine groups of cells within populations, comparing free cells, whose localized motion is relatively unrestricted by other members of the population, and caged cells, whose motion is highly restricted by neighboring cells.

1.3.3 – MDA-MB-231 Breast Cancer Cells

The type of cancer strain this research focuses on is endothelial breast cancer. MDA-MB-231 breast cancer cells receive their label from the patient the cells were originally harvested and cultured from. Breast cancer is notorious for being an aggressive cancer, as the cells are very motile and replicate very quickly, making it highly metastatic. Due to their active nature, breast cancer cells make for a strong representative cell type when studying endothelial cancer cell motion.[11] Figure 1.3 is a transmission microscopy image of a cultured MDA-MB-231 cancer cell population.

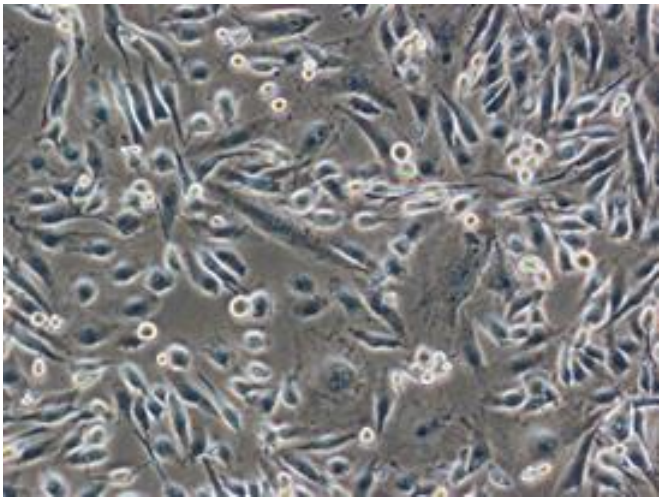

Figure 1.3 A microscopy image of MDA-MB-231 breast cancer cells.

Chapter 2 – Methods

2.1 - Cell Culturing and Staining

This research involves the use and study of live cell populations, therefore the growth and culturing of cells is necessary. Pre-cultured cells are removed from a 25-mm^2 flat-bottom flask by emptying out the present growth medium and adding 5 ml of a synthesized enzyme mixture known as TrypLE Select, which is designed to force the cells to de-adhere from the inner surface of the flask. After a period of about 10 minutes the mixture of freely suspended cells is transferred into a test tube. The test tube is then run through a centrifuge at 1000 RPM for 5 minutes to separate the cells from the TrypLE Select.

After being run through the centrifuge the TrypLE Select is removed from the test tube and 1 mL of growth medium added in. After thoroughly mixing the cells, 100 μL of the new mixture is added to a 25-mm^2 flat-bottom culturing flask containing 5 ml of standard cell growth medium. An additional 240 μL is used for the actual experiment, which is described in the next section.

This research relies on the fluorescence capabilities the laboratory's confocal microscope, so the cultured cells have two engineered retroviruses added to their flask. The first virus, BacMam GFP, is a modified insect virus that forces the host cell to produce proteins that adhere to the cytoplasm and cause it to fluoresce green under certain wavelengths of light. The second, Tubulin-RFP, forces cells to produce proteins that adhere to the nucleus and cause it to fluoresce red under certain wavelengths.

2.2 - Chemo Taxis Apparatus

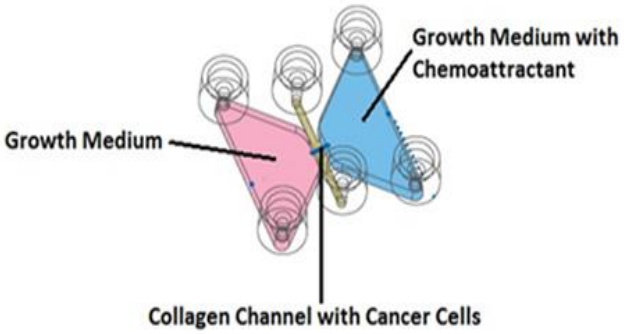

Figure 2.1 Diagram of chemo taxis apparatus. The device possesses two chemical reservoirs, both connected to a 1mm wide, 2mm long collagen channel. The reservoirs contain the growth medium and chemical attractant, creating the chemical gradient in the experiment. The channel houses the collagen network and the cell population being examined.

Cultured cancer cells stained with fluorescent markers are suspended in a liquid solution of type I collagen at a concentration of 9mg/mL. The solution is then drawn through a 1 mm wide 3D collagen channel connected to two chemical reservoirs, which is illustrated in figure 2.1. The process requires a vacuum channeling technique using two pipettes, as illustrated in figure 2.2. After the collagen solution has solidified, cell growth medium is added to the reservoirs, with the chemical attractant Fetal Bovine Serum (FBS) added to only one of them. The cells are

then free to move within the collagen under the influence of the established chemical gradient.

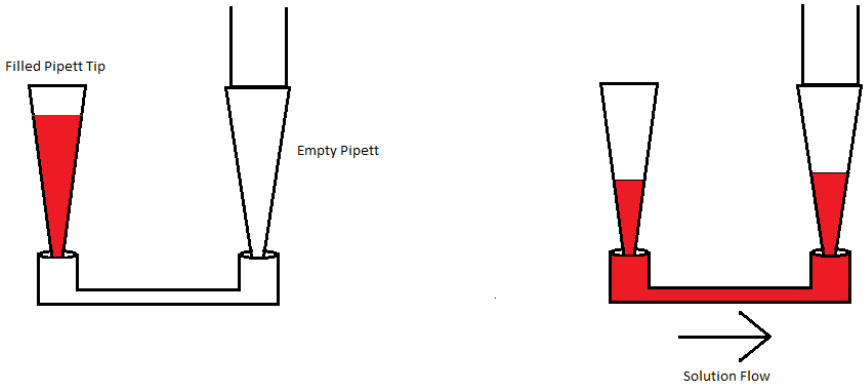

Figure 2.2 An illustration of the procedure necessary to place cell cultures within the main channel of the chemo taxis apparatus.

2.3 - Confocal Microscopy Imaging

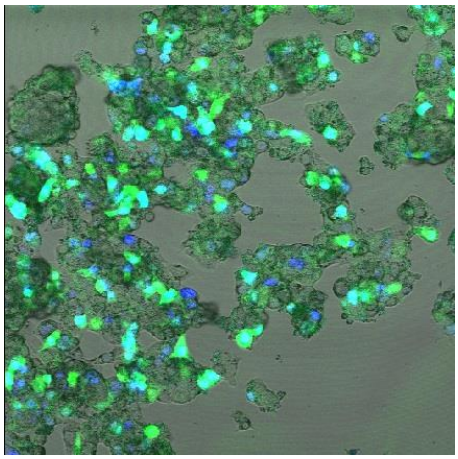

Figure 2.3 A confocal microscopy image of fluorescent cells. The BacMan GFP fluoresces the cells' cytoplasm and represented in this image as green. The Tubulin-RFP fluoresces the cells' nuclei, and is represented here as blue.

Once the experimental apparatus is set up the cells are ready to be imaged under the lab's confocal microscope. An on-stage thermal incubator is first setup on the microscope stage, set to average temperature of 37° C, and after placing the cells in the incubator, transmission light is used to find a large group cells representative of the whole population. The cells are then imaged under 490 nm green light and 600 nm red light, causing the cells' cytoplasm and nuclei to fluoresce. The microscope is then set to image the cells for 20 hours, taking an image once every 10 minutes. An image is only taken once every 10 minutes to keep the cells' exposure to the fluorescent light to a minimum, as too much exposure can kill them. After 20 hours the experiment is complete and the images are ready to be processed and analyzed. The images are run through a program designed to track the cells' trajectories. This data is then run through another program whose purpose is to analyze the data and process the cells' velocities, displacement, MSD and their velocity autocorrelation values.

2.4 – Image Processing and Data Analysis

After the experiment is complete the images captured at every 30 minutes are kept and used to analyze cellular motility. Those images are run through a manual tracking program, in which a user must go through each image, specifying to the program the locations of cells at each frame. The program then processes the data as trajectory values MATLAB is able to read.

When analyzing free and caged cells within the population, as each cell, when unelongated, had an approximate radius of 50 microns, a minimum radius of at least 150 microns of free space was decided the criterion to qualify as a free cell, and a maximum radius of about 50 microns of free space was decided as the criterion for a caged cell.

A custom created MATLAB script then interprets the data and uses it to calculate the trajectory, displacement, and velocity of all the cells in the population. It also plots the normalized velocity autocorrelation function of the cells, and their MSD. The script runs a curve fitting tool, fitting a single exponential decay to the autocorrelation plot, and from there calculating the fitted value of the persistence bias P.

The fitted value for the persistence bias is then used in Eq. 4. The parameter n is determined by the dimensionality of the collagen matrix, which in this research happens to be 3. The parameter S is defined as the speed of the cells, and since the cells have varying velocities with levels of periodicity, the average value of all the population's speed over the course of the experiment is used to fill that parameter.

Chapter 3 – Results

3.1 - Results of Cell Motion

3.1.1 – Cell Trajectory and Displacement

When collecting the results of the cell displacement, it was found that the cell populations, under the influence of the chemical gradient, displayed very biased directionally towards the higher concentration of the chemical attractant. To ensure this directionally was due to the established gradient and not an inherent feature of the cells themselves, a control group was also analyzed in which no chemical gradient was established. Figure 3.1 compares the experimental population and the control group, and as can as expected, the control group showed almost no directional bias, indicative of an isotropic random walk.

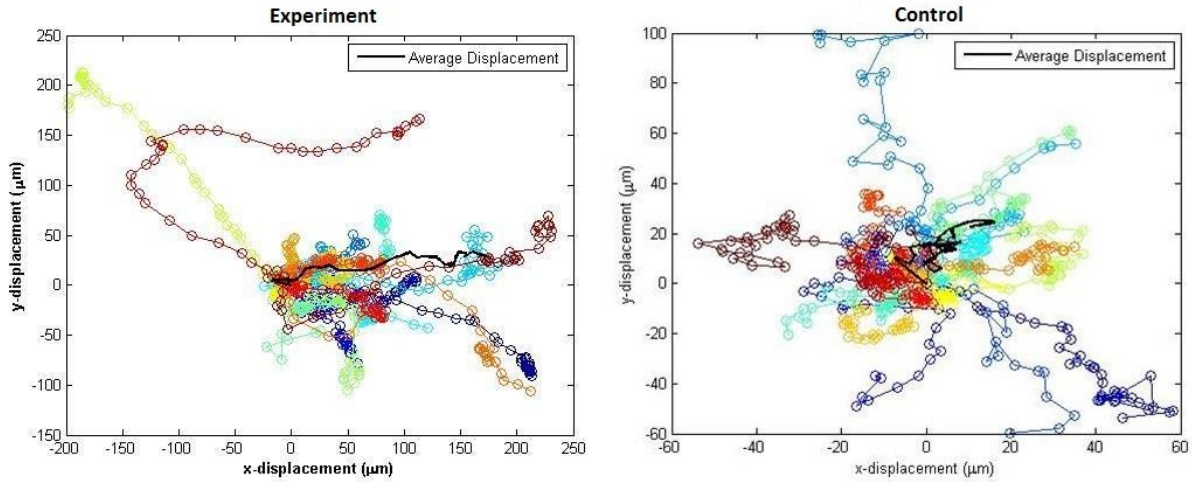

Figure 3.1 Shows cell displacement in both the experimental population with the chemical gradient, and the control group. In the experiment a population of 20 cells was analyzed and in the control group a population 15 cells were analyzed. Each colored line represents the displacement of an individual cell, while the solid black line represents the average displacement of the whole population. The direction of the chemical gradient is in the positive x direction.

The displacment of cells within the experimental population were also analyzed, comparing the trajectory of cells that were closer to the bulk of population, constrained by their neighbors, and cells that were in more sparse population clusters, with more space to move freely.

As can be seen in figure 3.2, both free and caged cells demonstrated directional motion, but only the caged cells showed motion in the direction of the chemical gradient.

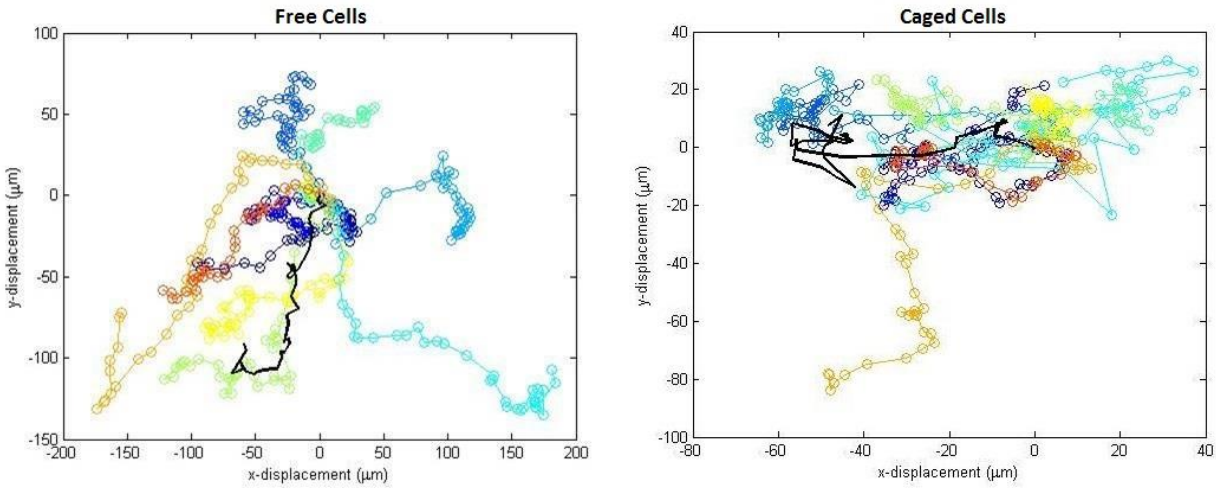

Figure 3.2 Shows cell displacement in both free cells and caged cells within a cancer population that had an established chemical gradient. In the experiment 8 free cells and 10 caged cells were analyzed. Each colored line represents the displacement of an individual cell, while the solid black line represents the average displacement of the whole population. The direction of the chemical gradient is in the negative x direction.

3.1.2 – Cell Velocity

Cell velocity was also analyzed, with the periodic velocity of cells in the direction of the gradient being plotted, as can be seen in figure 3.3. The cells velocities were very periodic due to their method of using pseudopods to travel, so an overall average speed was used when measuring the MSD. A slight decrease of overall speed over time was also noticed, mostly likely due a gradually weakening chemical gradient

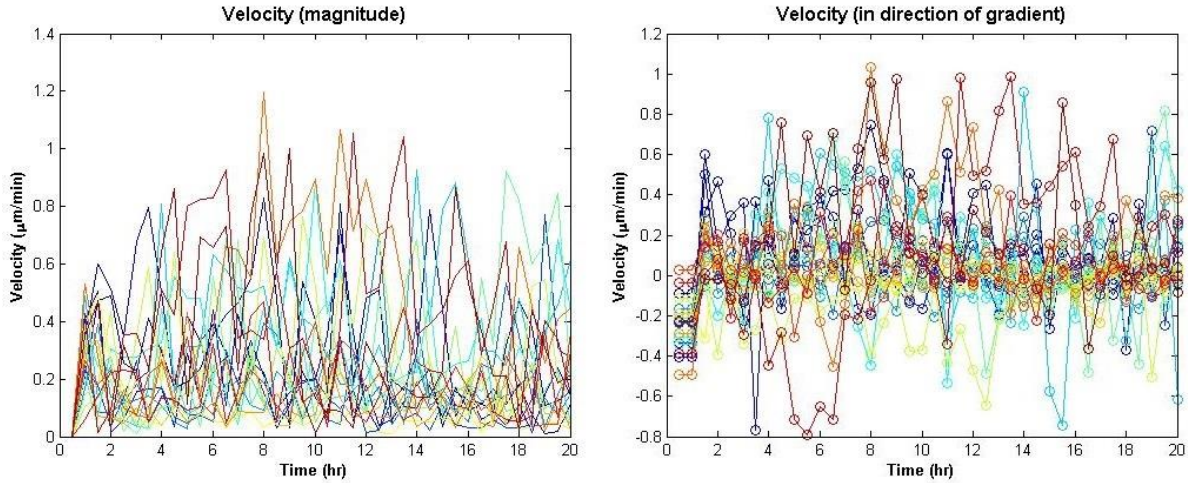

Figure 3.3 The first plot on the right represents the magnitude of the cells' velocities as a function of time. The second plot represents the velocity of the cells along the axis of the chemical gradient. Each colored line represents an individual cell.

3.2 – Velocity Autocorrelation and Mean Squared Displacement

The velocity autocorrelation and MSD of the general cell population were both processed, plotted, and compared the theoretical values predicted by the model of a PRW. In Figure 3.5 both the velocity autocorrelation and MSD of the cancer cell population are plotted against the predictions of a PRW. The autocorrelation fit has an R^2 value of about 0.81, indicating a fairly good fit. The MSD fit has an R^2 value of about -1.3, indicating massive discrepancies between the model and the experimental data.

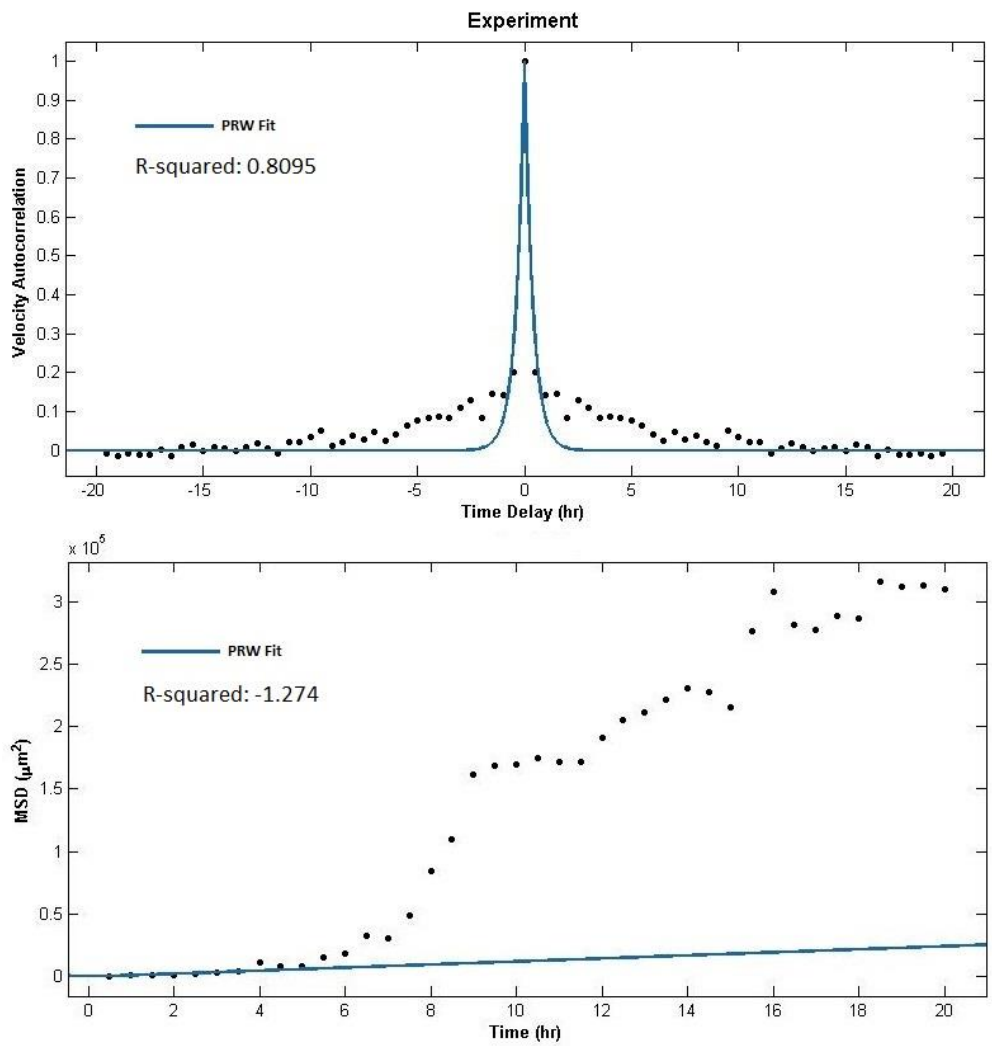

Figure 3.4 The first plot is the velocity autocorrelation of the cell population, with the decaying exponential predicted by the PWR fitted to the data. According to the fit the persistence bias P was approximately 20.1 minutes. In the second plot the calculated persistence bias was used to fit the PRW model's MSD to that of experimental results. Average velocity for this population of cells was approximately 0.32 μm/min.

Again, cells within the population were analyzed, comparing free and caged cells within the population. For both free and caged cells the velocity autocorrelation function modeled by the PRW was fitted to the experimental results. As can be seen in Figure 3.6, the autocorrelation fit for the free cell population has an R^2 value of approximately 0.86, and for the caged cell population the R^2 value is about 0.91, indicating strong correlation experiment and theory.

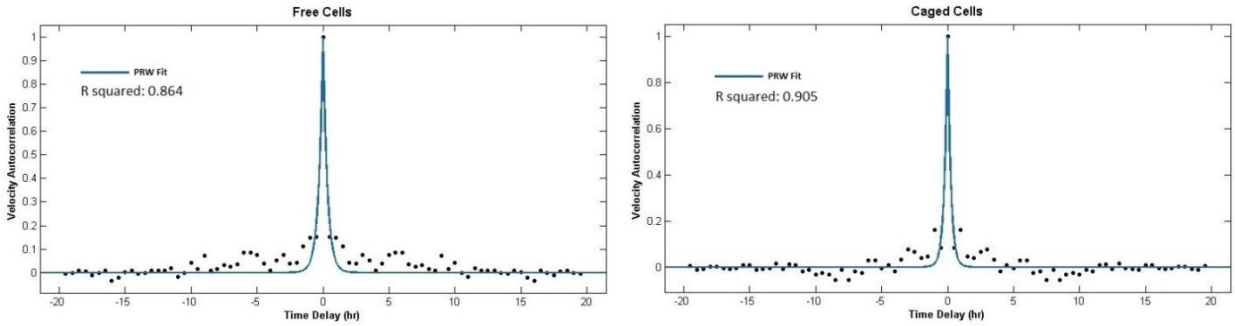

Figure 3.5 Shows the velocity autocorrelation plots of free cells and caged cells within a population, with the velocity autocorrelation modeled from the PWR fitted to the experimental values. According the fitted model, the persistence time for the free cells was approximately 19.4 minutes, and for the caged cells it was approximately 14.4 minutes.

Using the persistence bias values obtained from the autocorrelation fits, the MSD function modeled in the PRW was fitted to the populations' MSD values, as can be seen in Figure 3.7. The free cell population and caged cell population had R^2 values of -1.41 and 0.08, respectively. This indicates little no correlation between the theorized model and the actual data.

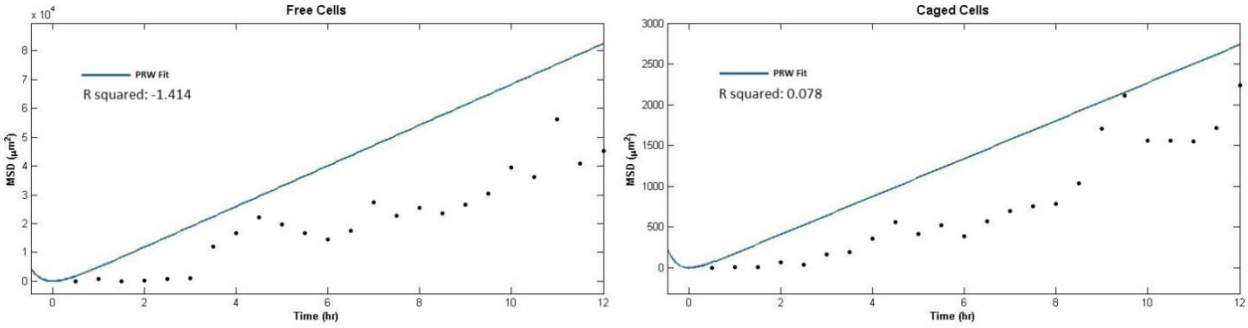

Figure 3.6 Shows the MSD plots of free cells and caged cells within a population, with MSD modeled from the PRW fitted to experimental values using the persistence bias measured from the autocorrelation function, and the cells' average velocity. For the free cells the average velocity was approximately 1.42 µm/min, and for the caged cells it was about 0.3 µ/min. Only the first 12 of the experiment was examined, as the MSD trend progressively deteriorated at later times.

Chapter 4 – Discussion

4.1 – Comparison of Breast Cancer Cell Chemo taxis to the model of a Persistent Random Walk

When analyzing the overall displacement of the experimental breast cancer cell population, it showed clearly directionality in the direction of the chemical gradient, indicating a bias in the motion of the population, something a persistent random walk should be able to accurately model. When processing the normalized velocity autocorrelation of the cancer cell population, the plotted data was distributed in the shape of a simple decaying exponential, following the function modeled by the PRW.

The fit showed a relatively fair correlation with the experimental data, having an R^2 value of about 0.81. From this fit the persistence bias of the population could be calculated, and be used to fit the modeled MSD to measured data. Despite the similarities exhibited between experiment and theory when plotting the velocity autocorrelation, the MSD showed no such similarities.

Theory and data in the MSD showed very strong correlation in the first 5 to 6 hours, but after 6 hours the measured results quickly deviated from prediction, taking a sharp exponential increase. The R^2 value for the MSD fit was -1.274. Negative R^2 values usually indicate a model that is unable to fit your measured data, lending evidence towards the idea that the model of a PRW is insufficient in modeling endothelial cancer cell motion.

Free and caged cells within the population were also examined and it was surprising to see just how well the PRW's velocity autocorrelation fitted to that of actual data, free and caged cells having R^2 values of 0.86 and 91 respectively. It made it that much more surprising that the PRW fit for the MSD showed little to correlation with measured data. The MSD fits for the free and caged cells had R^2 values of -1.41 and 0.8 respectively, both extremely poor fit values, lending further credence to the thought that the model of a PRW may be outdated, at least for breast cancer cells.

Chapter 5 – Conclusion

In conclusion, though breast cancer chemo taxis demonstrates strong bias, evidence shows that its collective motion may not be able to be modeled by the application a persistent random walk. The fact that the velocity autocorrelation and MSD modeled by the PRW disagree with each other so much when applied to a population of breast cancer cells lends evidence that model itself may break down when applied to cancer motion and metastasis.

5.1 – Future Research

Possible future research would be to perform this research again, examining much larger populations of cells, studying whether or not the PRW model works again if the population is large enough. Application of this research to other cancer cell types is another path of study that could be taken. Lastly, and most importantly, is development of a possible model of motion that better models collective cancer motion.

Bibliography

1. Tranquillo, RT., Lauffenburger, DA., Zigmond, SH. “A stochastic model for leukocyte random motility and chemotaxis based on receptor binding fluctuations.” *J Cell Biol.***106(2)**:303–309 (1988).

2. Wu, PH., Giri, A., Wirtz, D. “Statistical analysis of cell migration in 3D using the anisotropic persistent random walk model.” *Nature Protocols* **10**,517–527 (2015).

3. Berg, HC. “Random Walks in Biology.” *Princeton*: Princeton Univ Press; 1993.

4. Haeger, A., Krause, M., Wolf, K., & Friedl, P. “Cell jamming: Collective invasion of mesenchymal tumor cells imposed by tissue confinement.” *Biochimica Et Biophysica Acta (BBA) - General Subjects* **1840(8)**, 2386–2395 (2014).

5. Marel, AK., et al. “Flow and Diffusion in Channel-Guided Cell Migration.” *Biophysical Journal* **107(5)**, 1054-1064 (2014).

6. Hanahan, D., Weinberg, RA. “Hallmarks of cancer: The next generation.” *Cell*, **144(5)**: 646–674 (2011).
7. Codling, AC., Plank, MJ., Benhamou, S. “Random walk models in biology.” *J R Soc Interface*; **5(25)**: 813–834 (2008).
8. Stokes, CL., Lauffenburger, DA., Williams, SK. “Migration of individual microvessel endothelial cells: Stochastic model and parameter measurement.” *J Cell Sci*; **99(Pt 2)**:419–430 (1991).
9. Fraley, SI., Feng, Y., Giri, A., Longmore, GD., Wirtz, D. “Dimensional and temporal controls of three-dimensional cell migration by zyxin and binding partners.” *Nat Commun*; **3**:719 (2012).
10. Liu, L., Duclos, G., Sun B., Leed J., Wue A, Kamf Y, Sontagg ED, Stonec HA, Sturme JC, Gatenby RA, Austin RH. “Minimization of thermodynamic costs in cancer cell invasion.” *PNAS*. **110(5):** 1686-1691 (2013).
11. Hunter, KW., Crawford, NP., Alsarraj, J. “Mechanisms of metastasis.” *Breast Cancer Res*; **10(Suppl 1)**:S2 (2008).